

AD-A104 403 CENTRE NATIONAL DE LA RECHERCHE SCIENTIFIQUE BESANCO--ETC F/G 14/2
LOW TEMPERATURE QUARTZ CRYSTAL OSCILLATOR FAST WARM-UP SAW OSCI--ETC(II)
JUL 81 J J GAGNEPAIN, D HAUDEN AFOSR-80-0105

UNCLASSIFIED

RADC-TR-81-184

NL

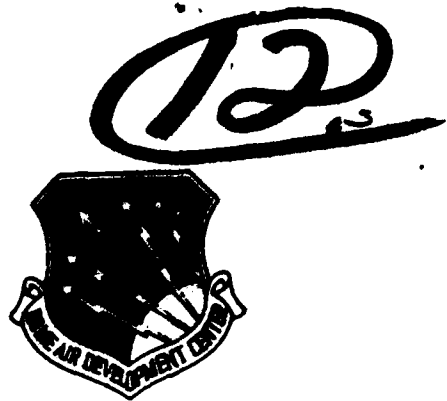
100
20
AD-403

END
DATE
10-81
DTIC

AD A104403

RADC-TR-81-184
Interim Report
July 1981

LEVEL



LOW TEMPERATURE QUARTZ CRYSTAL OSCILLATOR FAST WARM-UP SAW OSCILLATOR

Lab de Physique et Metrologie des Oscillateurs

J. J. Gagnepain
D. Heudon

APPROVED FOR PUBLIC RELEASE; DISTRIBUTION UNLIMITED

DTIC
ELECTE
SEP 21 1981
S D
D

ROME AIR DEVELOPMENT CENTER
Air Force Systems Command
Griffiss Air Force Base, New York 13441

0500 FILE COPY

81 9 21 056

This report has been reviewed by the RADC Public Affairs Office (PA) and is releasable to the National Technical Information Service (NTIS). At NTIS it will be releasable to the general public, including foreign nations.

RADC-TR-81-184 has been reviewed and is approved for publication.

APPROVED:



NICHOLAS F. YANNONI
Project Engineer

APPROVED:



FREEMAN D. SHEPHERD, JR.
Acting Director
Solid State Sciences Division

FOR THE COMMANDER:



JOHN P. HUSS
Acting Chief, Plans Office

If your address has changed or if you wish to be removed from the RADC mailing list, or if the addressee is no longer employed by your organization, please notify RADC (ESE) Hanscom AFB MA 01731. This will assist us in maintaining a current mailing list.

Do not return this copy. Retain or destroy.

UNCLASSIFIED

~~SECURITY CLASSIFICATION OF THIS PAGE (When Data Entered)~~

DD FORM 1 JAN 73 1473 EDITION OF 1 NOV 68 IS OBSOLETE

UNCLASSIFIED 3743
SECURITY CLASSIFICATION OF THIS PAGE (When Data Enclosed)

CLASSIFIED

394359

UNCLASSIFIED

SECURITY CLASSIFICATION OF THIS PAGE(When Data Entered)

to the 4th power

① The measurements of the frequency noise of different quartz resonators at room temperature show a correlation between $1/f$ noise levels and Q-factors, following a $1/Q^4$ law. This new property was confirmed by measuring the $1/f$ noise level of a pair of resonators at 300 K, 4.2 K and 1 K.

A first theoretical study enables to explain the $1/Q^4$ law from the phonon-phonon interactions due to the crystal anharmonicities.

② Under fast temperature variations frequency shifts are observed in SAW delay lines, which are proportional to the time derivative of the temperature. This dynamic thermal behavior was evaluated for ST cut quartz and found comparable to that one of AT-cut quartz BAW resonators. Therefore such a thermal sensitivity is not admissible for fast warm-up oscillator applications and must be lowered.

Accession For	
NTIS GRA&I	<input checked="" type="checkbox"/>
DTIC TAB	<input type="checkbox"/>
Unannounced	<input type="checkbox"/>
Justification	
By _____	
Distribution/	
Availability Codes	
Dist	Avail and/or Special
A	

DTIC
SELECTED
SEP 21 1981
S D

D

UNCLASSIFIED

SECURITY CLASSIFICATION OF THIS PAGE(When Data Entered)

LOW TEMPERATURE QUARTZ CRYSTAL OSCILLATOR

FAST WARM-UP SAW OSCILLATOR

Table of Contents

Acknowledgements	iv
I - Low Temperature quartz crystal oscillator	
General presentation	1-1
Cryogenic equipment	1-2
Crystal parameters at low temperature	1-3
I/F noise measurements	1-5
Theoretical approach	1-15
Conclusion	1-23
References	1-24
II - Fast warm-up SAW oscillator	
General presentation	2-1
Temperature distribution	2-2
Frequency shifts	2-4
Temperature controlled oven	2-7
Experimental results	2-8
Conclusion	2-10
References	2-10

ACKNOWLEDGEMENTS

The theoretical study of $1/f$ noise fundamental mechanisms was performed with valuable contribution of Prof. J. Uebersfeld of Université P. et M. Curie and of L.P.M.O. Authors also are indebted to Prof. P.H. Handel of Saint Louis Missouri State University for helpfull and stimulating discussions on the $1/f$ quantum theor

Contributions of various portions of the program were made by the following staff members of L.P.M.O.

Mrs G. Théobald
MM. G. Goujon
J. Groslambert
C. Paulin
R. Brendel

I - LOW TEMPERATURE QUARTZ CRYSTAL OSCILLATOR

GENERAL PRESENTATION

The frequency stability of quartz oscillators is affected by

- the noise of the electronics : thermal noise and 1/F noise
- the peculiar frequency noise of the resonator : frequency random walk noise and 1/F noise.

When the noise of the electronics is reduced at the lowest possible level compatible with the state of the art of electronic components, the limit of stability of the oscillator corresponds to the resonator noise.

- the frequency random walk is essentially due to temperature fluctuations ⁽¹⁾ and can be reduced by using high quality temperature controlled ovens ⁽²⁾.

- the 1/F noise level indeed defines the ultimate limit of stability. To the 1/F spectrum of the frequency domain corresponds a floor, the flicker floor, in the time domain.

It was known that at very low temperature the internal losses and the acoustic attenuation of quartz material are reduced and therefore the Q-factor of resonators is increased.

The present work shows that

- the 1/F noise level at room temperature is correlated with the Q-factor, following a $1/Q^4$ -law.
- at low temperatures it is possible to minimize, by at least one order of magnitude, the 1/F noise level. Improvement of the frequency stability follows.

The study of the noise levels as a function of temperature required

- cryogenic equipment operating at 1°K
- test set for crystal adapted to very high Q's and low motional resistances
- frequency noise measurement system for pairs of resonators at 300°K and 1°K.

1/F noise is an universal noise, which can be observed in almost all physical phenomena and systems. Its origin and mechanisms are not known. A theoretical study has been undertaken, and the first task was to explain the $1/Q^4$ dependence law, which was experimentally demonstrated.

CRYOGENIC EQUIPMENT

A liquid helium dewar with double isolation was used. Its capacity is 5 and gives an autonomy of one or two days, depending on the number of leads and cables sunk in it. This small size was chosen in order not to expend to much liquid helium when the different quartz samples successively are cooled and heated. In the second phase of the project a 30 liters dewar will be used to maintain Xtal oscillators below 4K during periods of time of the order of several weeks. Vacuum pumps enable to reach temperatures between 4.2K and 1K. Temperature is measured by means of carbon and germanium resistors, and also by means of the bath pressure when below 4.2K.

For guide measurements, the resonators are directly sunk in the helium bath. If more stability, mainly versus temperature, is required they are enclosed in a copper can.

This cryogenic equipment was ready to use in February 1980.

CRYSTAL PARAMETERS AT LOW TEMPERATURE

The measurements were performed by using the π transmission method.

Measurement system

Measurements at low temperature present some difficulties because of the length of the cables between the resonator at the bottom of the dewar and the source and detector which are at room temperature. Therefore it is necessary to place the π network with the resonator in the bath.

The test set is represented on fig. 1.

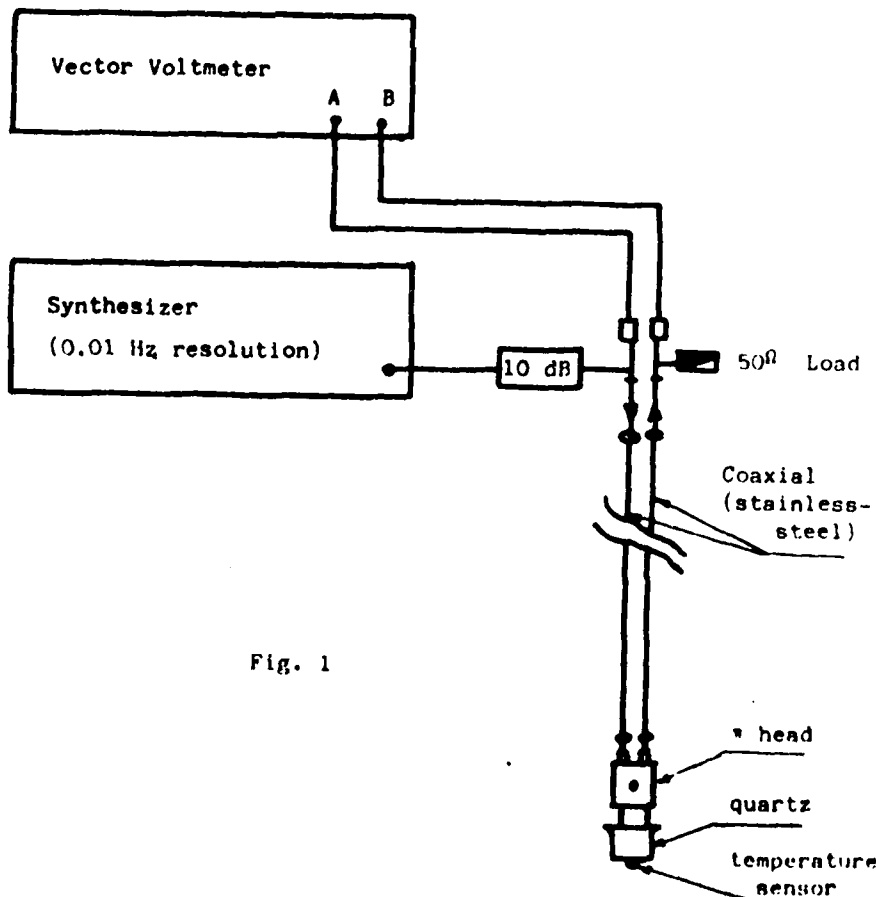


Fig. 1

The π network must be adapted to 50Ω , the characteristic impedance of the cables. But the values of the parallel resistors must be chosen as a function of the motional resistance R_1 of the resonator. This last one can become close to 1Ω at very low temperature. Therefore two π networks were used. Their values are given on fig. 2a and 2b.

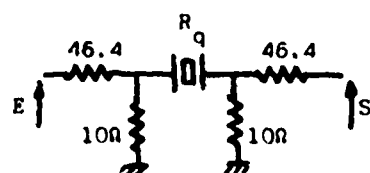


Fig. 2a : $50 \Omega < R_1 < 400 \Omega$

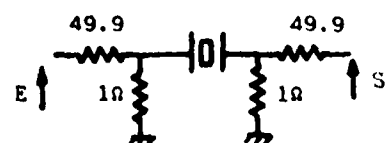


Fig. 2b : $0.1 \Omega < R_1 < 20 \Omega$

The π network head must be constructed with care. To avoid spurious contact resistances at temperatures below 4K all the electrical contacts were gold plated. The π head is represented on fig. 3.

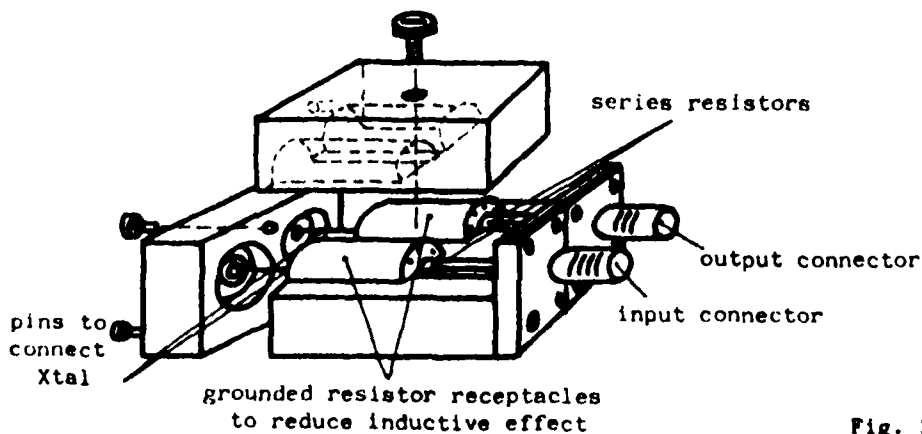


Fig. 3

Frequency, motional resistance and Q-factor were measured between 1K and 20K. This temperature range corresponds to the diminution of the acoustic attenuation, the phonon-phonon interaction peak being located at 20K.

The highest Q-factor was obtained with G4 and corresponds to $Q = 150 \cdot 10^6$ at $T = 1.5K$.

The Q and R_1 values of the resonators provided by RADC are shown on fig.4 and 5.

The corresponding frequency shifts are given on fig. 6. They are of the order of 5 to 6 KHz. the temperature coefficient of the frequency was also measured. It decreases with temperature, as expected (fig. 7).

At room temperature, the Q -factor values of these resonators are closed. But at low temperature a large dispersion is observed. The inverse Q -factor can be written

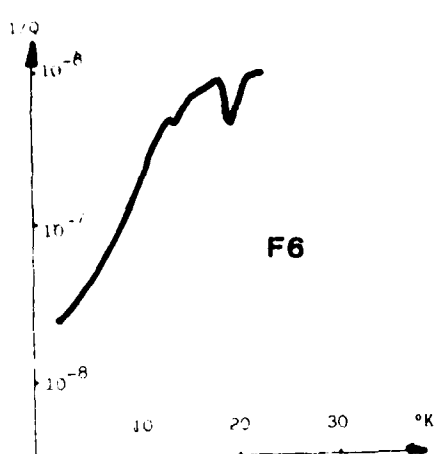
$$1/Q = 1/Q_b + 1/Q_s + 1/Q_e$$

This relation points out the different loss contributions due to the crystal bulk ($1/Q_b$), the surface ($1/Q_s$) and the environment ($1/Q_e$) constituted of the electrodes and the mounting. $1/Q_b$ is representative of the crystal properties and depends on the phonon interaction processes. Its contribution is predominant at 20°K and certainly also at room temperature. $1/Q_b$ decreasing with temperature as T^4 it becomes negligible at low temperature. The influence of $1/Q_s$ and $1/Q_e$ appears and leads to a threshold. These two last contributions are mainly representative of the resonator technology.

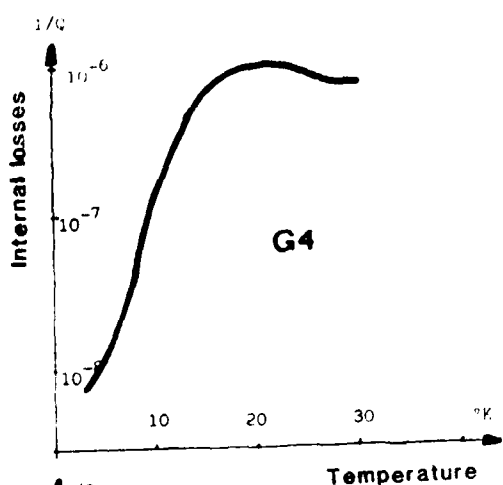
1/F NOISE MEASUREMENTS

1) Room temperature

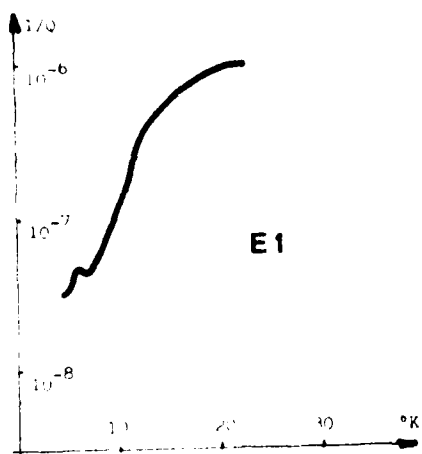
The $1/f$ frequency noise of resonators cannot be measured in an oscillating loop, because the phase fluctuations of the loop due to the electronics are generally higher. The method which is used consists in driving in a π transmission network two identical resonators by means of a frequency source with high spectral purity ⁽³⁾⁽⁴⁾. Identical resonators means resonators with identical frequencies and Q -factors, or made identical with tuning capacitors and resistors. Therefore a preselection of pairs of resonators at the same frequency is necessary. The measurement system is shown on fig. 8.



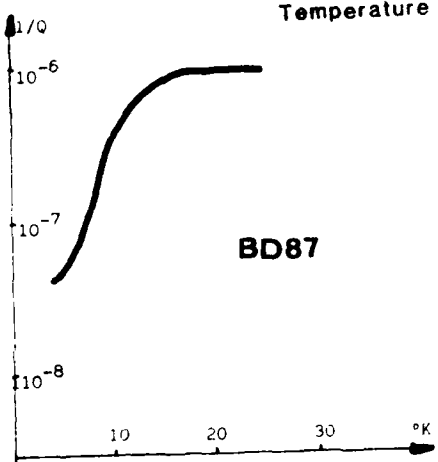
F6



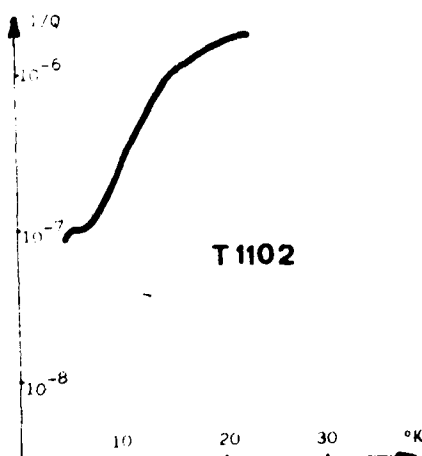
G4



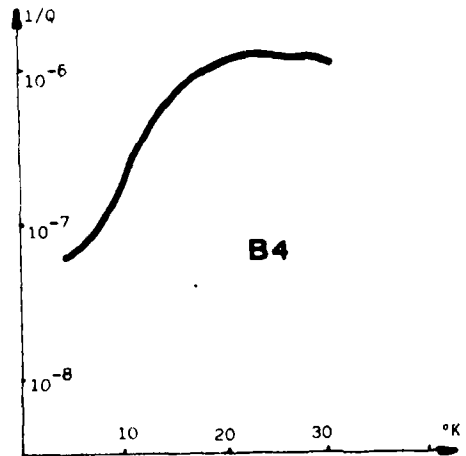
E1



BD87



T1102



B4

Fig. 4
1-6

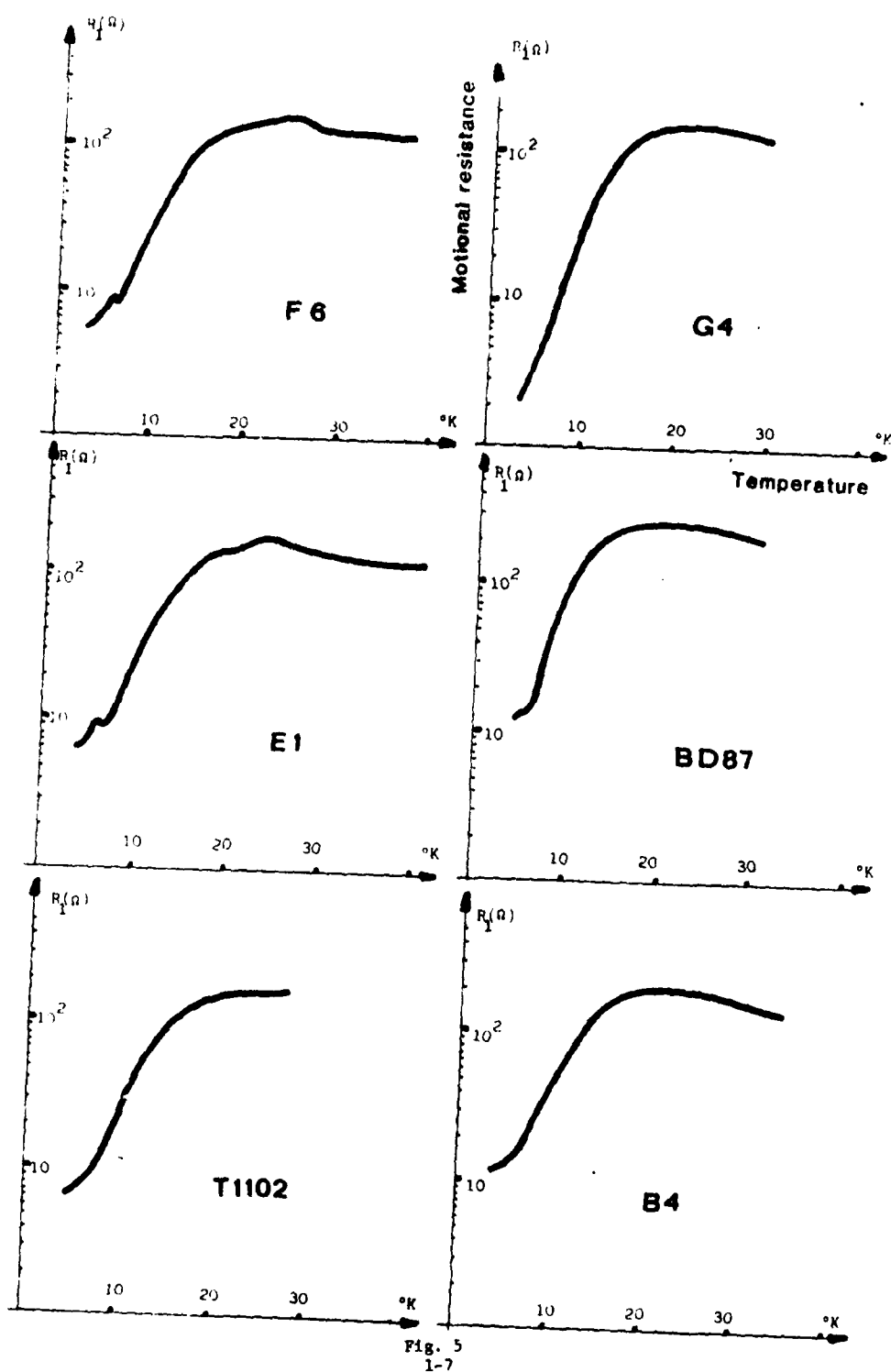
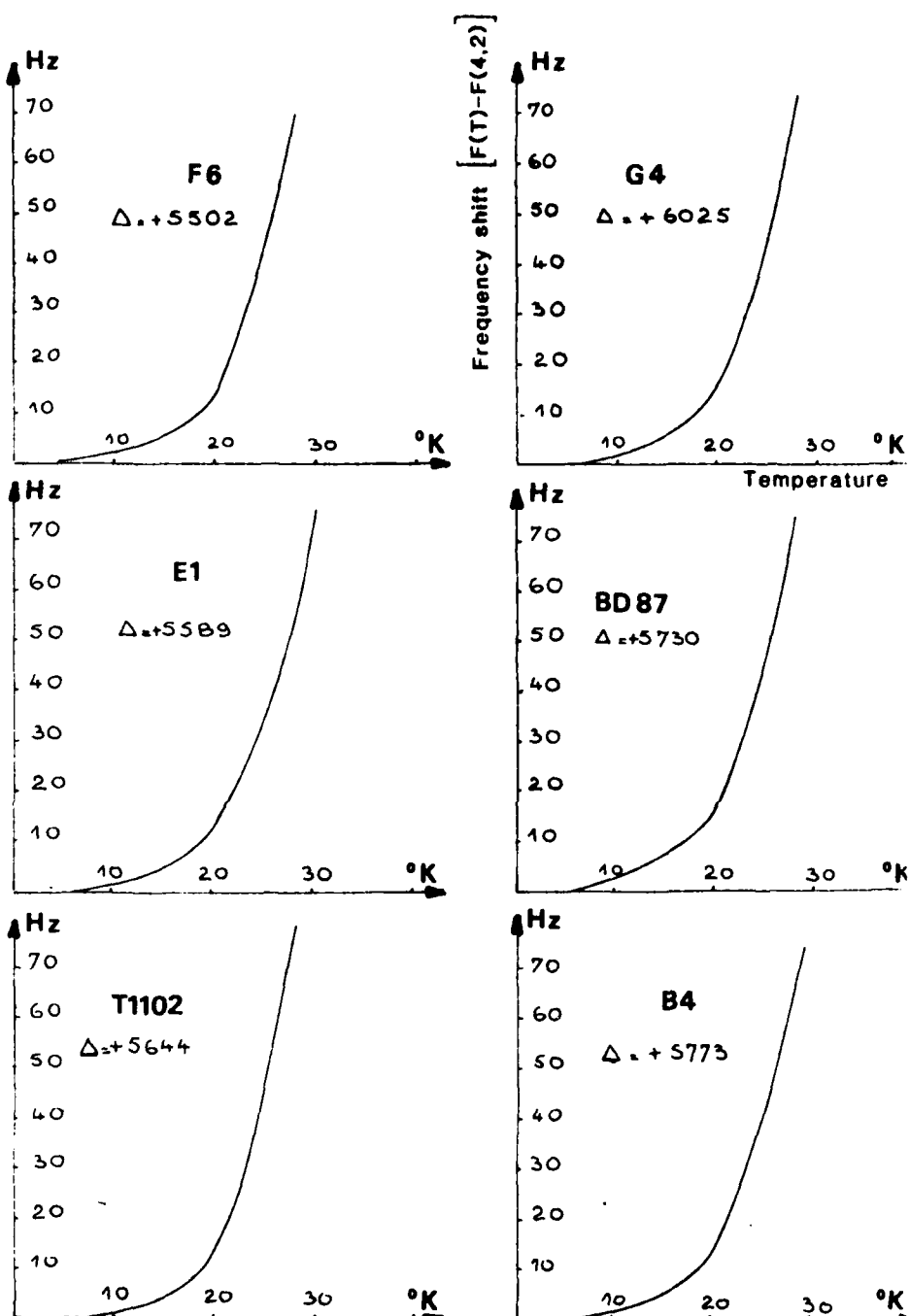


Fig. 5
1-7



$$\Delta(\text{Hz}) = F(300^\circ\text{K}) - F(4.2^\circ\text{K})$$

1-8

Fig 6

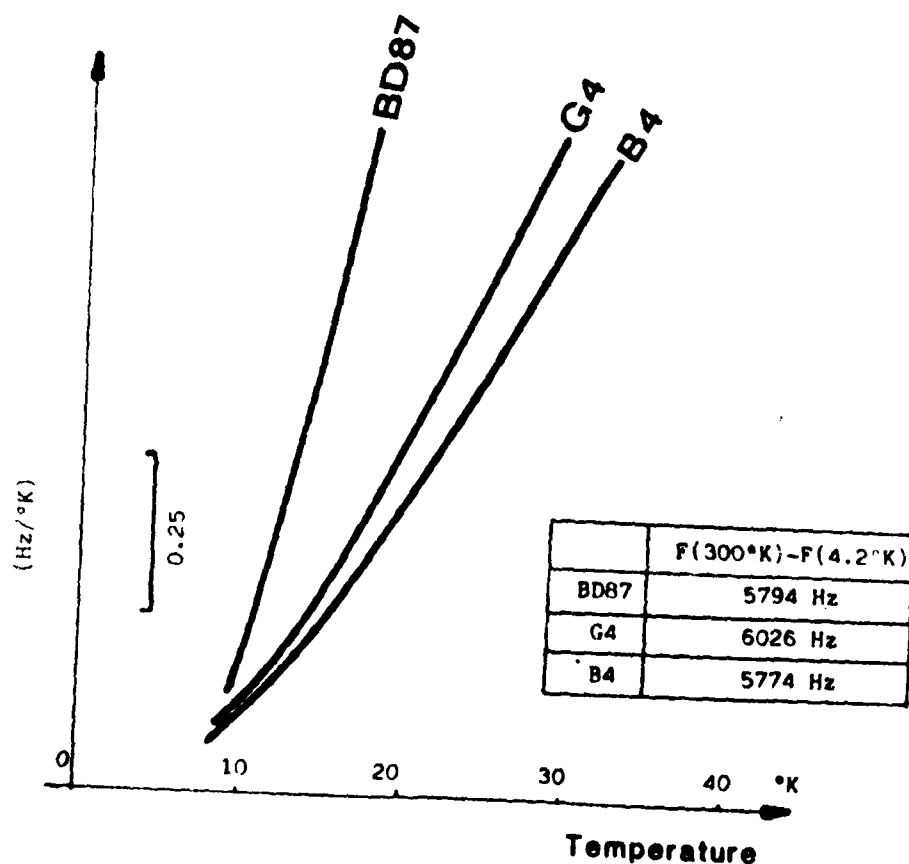
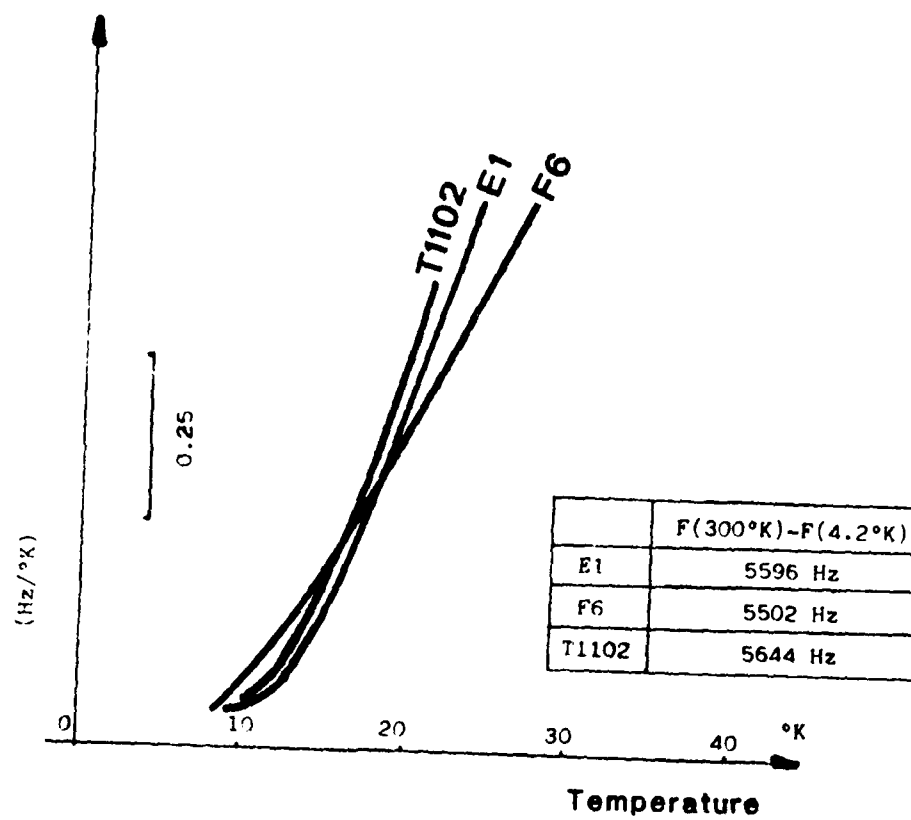


Fig. 7
1-9

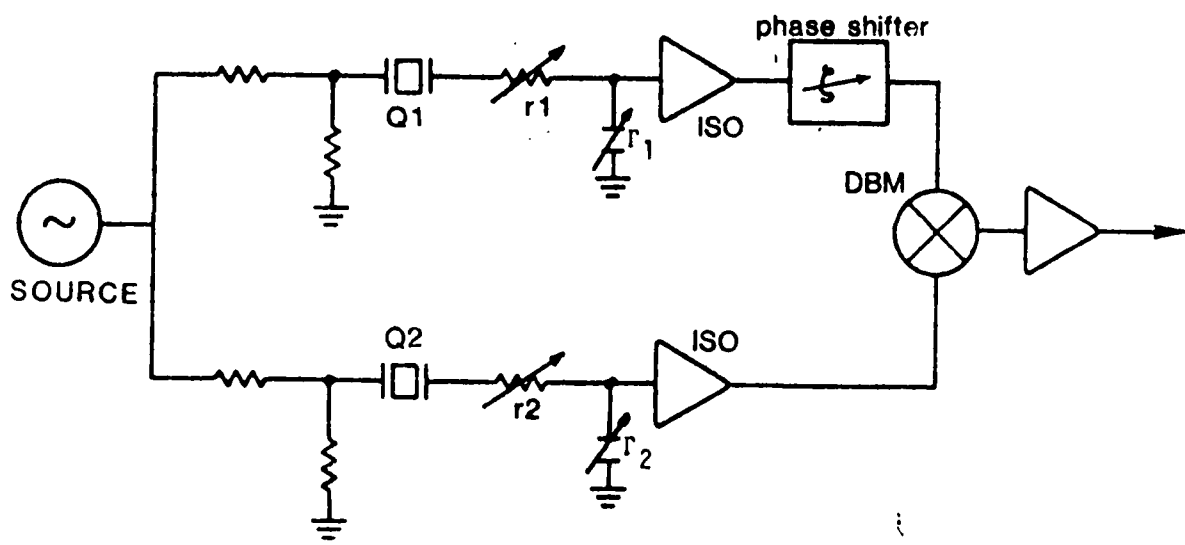


Fig. 8

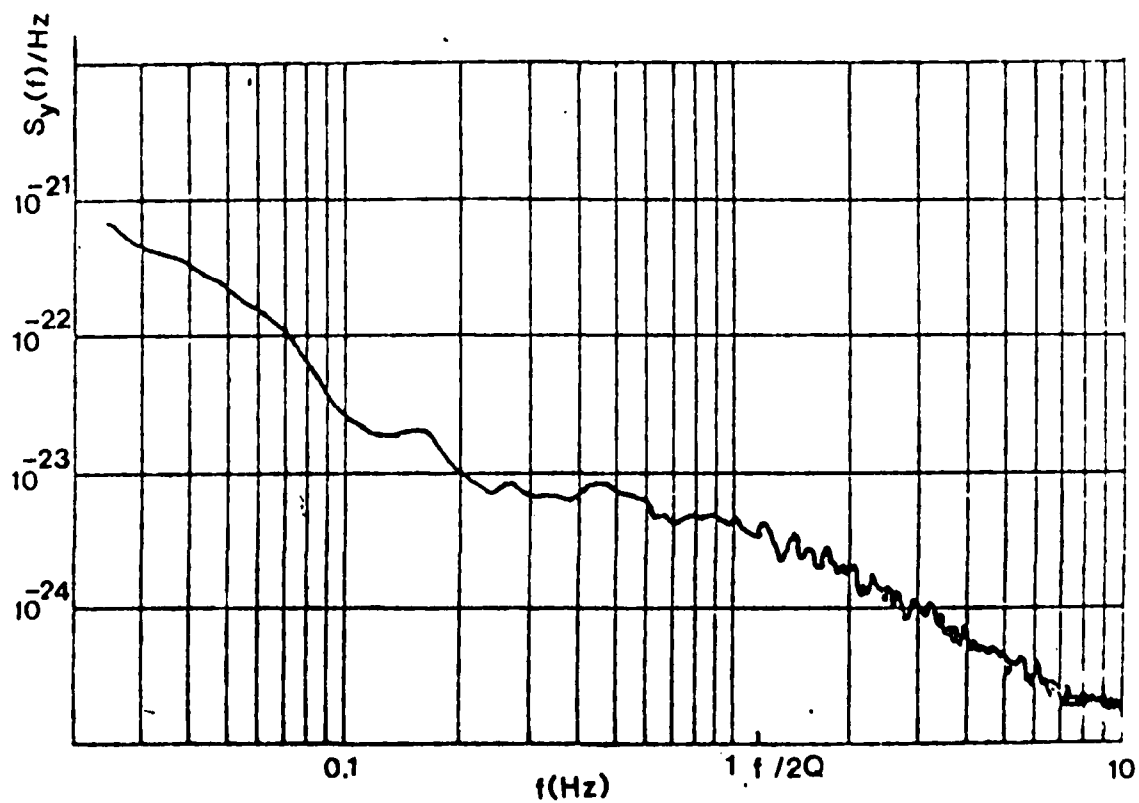


Fig. 9
1-10

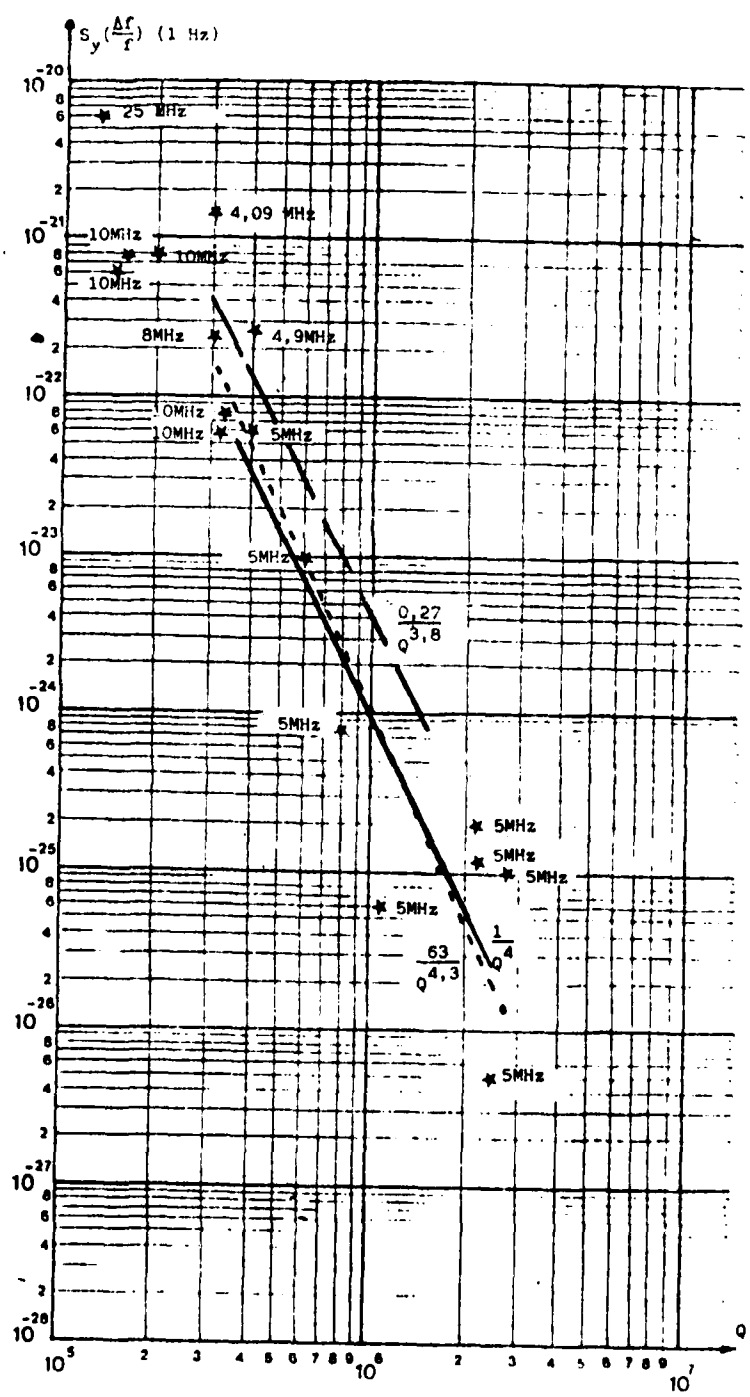


Fig. 10
1-11

When the two arms of the phase bridge are correctly balanced 50 dB to 60 dB of rejection of the source frequency fluctuations are obtained.

The resolution depends on the resonators Q-factors following the relation between the phase and frequency fluctuations $d\phi = -2Q df/f$, for Fourier frequencies within the resonator's bandwidth.

On fig. 9 is shown a typical frequency noise spectrum. Three different noises appear : frequency random walk ($1/f^2$) for the lowest Fourier frequencies flicker noise ($1/f$) for the intermediate ones and white noise (F^0) for the highest ones. $1/f^2$ noise is related to the crystal temperature fluctuation ΔT through its dynamic thermal coefficient α following the law $\Delta f/f = \alpha \Delta T/\Delta t$ ⁽³⁾. This noise can be minimized by using thermostats with high accuracy. For ΔT cut α is $10^{-5} \text{ s}/^\circ\text{C}$. This means that the achievement of a 10^{-13} frequency stability needs a temperature control as good as $10^{-8} \text{ }^\circ\text{C/s}$.

The white noise which is observed has nothing to do with the resonators, but is due to the measurement system itself.

The level of $1/f$ noise was measured for a large number of pairs of resonators at different frequencies, and with a large dispersion of the Q-factor values. On fig. 10 are plotted the different noise levels measured on all those resonators and given at 1 Hz from the carrier.

From these experimental data the dependance between $1/f$ noise and Q-factor is determined by using a regression method (linear regression with the logarithmic scales). This leads to the general relation

$$S_y(f) = \frac{\lambda}{Q^n} \frac{1}{f}$$

The values obtained for n and λ depend on the selection of the experimental points among the 18 available values. After mathematical treatment it can be shown that $3.8 \leq n \leq 4.3$. Therefore it is proposed to consider that the most probable value will be $n = 4$. A small variation in the n value induces a drastic change of the constant λ , and for the previous range of n the corresponding values of λ are $0.1 < \lambda < 60$. A reasonable fitting will correspond to λ close to unity when n is made equal to the integer 4.

2) Low temperatures

At room temperature there is no way for modifying the Q-factor of one resonator. An additional resistor will change the loaded Q, but not the unloaded one which is relevant for the noise measurements. The only possibility was to use different resonators with different unloaded Q-factors.

But the acoustic attenuation is strongly dependent of temperature at low temperatures and can be either increased near the phonon-phonon interaction peak and near the impurity relaxation peaks, or decreased for temperatures below 10K as it has been shown.

The previous noise measurement system, which requires a pair of resonators at the same frequency, is not adapted for low temperature measurements. The frequency variations from 300K to 4K are of the order of a few KHz. But because of small differences in the crystal orientation, this frequency variation versus temperature is not reproducible enough. Even when identical at room temperature, the frequencies of a pair of resonator present differences of several 100 Hz which cannot be cancelled out by using tuning external capacitors.

Therefore a new measurement system for low temperatures was studied. Its schematic diagram is represented on fig. 11.

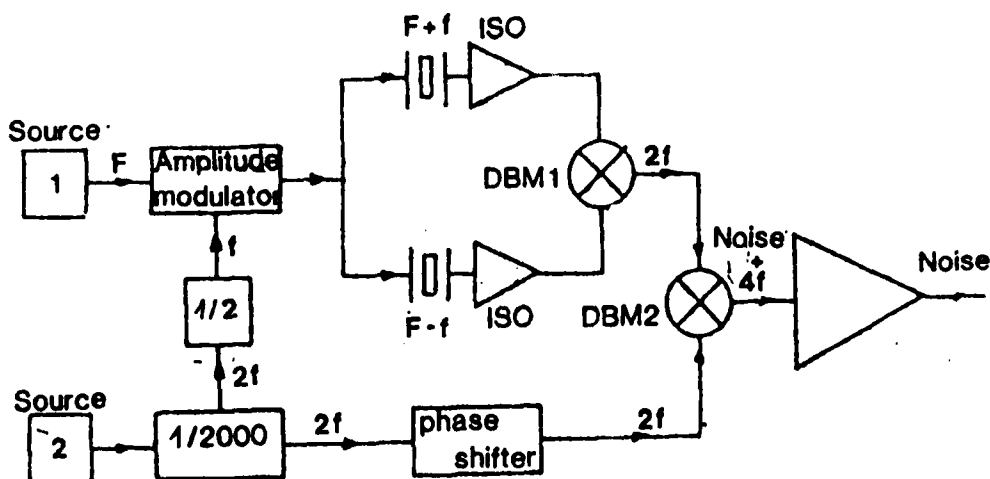


Fig. 11

Each of the two resonators is excited by one of the side bands of an amplitude-modulated signal (without carrier). At the output of the first mixer the intermediate frequency is affected by the total frequency noise of the resonators. The influence of the driving source is cancelled out by balancing the characteristics of the resonators. It is necessary to use a good frequency source for the modulating signal, even if its frequency spectrum is purified by dividing by 4000.

The first mixer is followed by a low noise amplifier, with 20 dB of gain.

A second mixing with a $2f$ reference frequency delivered from a digital phase shifter coupled to the divider gives a noise voltage proportional to the resonator's frequency fluctuations. A filter-amplifier cancels out the $4f$ frequency component. A FFT spectrum analyzer gives directly the $S_y(F)$ spectrum of the two resonators.

One other advantage of such a measurement system, when compared to the previous one, is to enable easier and faster calibration, just changing by a small amount the modulation frequency and measuring the DC voltage shift at the mixer output.

The $1/F$ noise of a pair of identical AT-cut quartz resonators (manufactured by CEPE) were measured at 300K, 4.2K and at 1K. The frequency difference between the two resonators was 1 KHz. The noise levels for one resonator are given on table I.

Temperature	300°K	4.2°K	1°K
Q	$2.4 \cdot 10^6$	$5 \cdot 10^6$	$9 \cdot 10^6$
$S_y(1 \text{ Hz})$	$1.6 \cdot 10^{-24}$	$1.4 \cdot 10^{-25}$	$3.5 \cdot 10^{-26}$

Table I

These results confirm the dependence of $1/F$ noise on Q-factor and in this case with the same resonator. The data does not follow strictly the $1/Q^4$ law. A comment on this point will be given in the next section.

THEORETICAL APPROACH

It is known that the acoustic attenuation results from the interaction of the sound wave with the thermal phonons of the crystal. This is a fundamental phenomenon, which would appear even in a perfect crystal, i.e. without defects, because of the anharmonicities of the lattice, due to the nonlinear nature of the interatomic bonds. Also because of these nonlinearities are modifications of the phonon frequencies and of the sound wave velocity.

Calculations of attenuation were made by using two different theoretical approaches. In the Landau and Rumer theory (1937) ⁽⁵⁾ the sound wave is considered as a beam of phonons which are scattered by collisions with the thermal phonons. This theory does not take into account the interactions between thermal phonons and is valid only in the low temperature range, when the phonon life time and mean free path are large and therefore energy and momentum are well defined. At higher temperatures the life time becomes shorter. The uncertainties of energy and momentum increase and the selection rules arising from energy and momentum conservation laws break down. In the second theory due to Akhieser (1939) ⁽⁶⁾ the sound wave is represented macroscopically (and not microscopically as in the Landau-Rumer theory). The thermal phonon system is disturbed from equilibrium by the sound wave strain but tends to return to equilibrium because of the collisions between thermal phonons. In this case the phonons are localized and their mean free path has to be small when compared to the sound wave length.

1) Harmonic approximation

The main results of the lattice dynamics in the harmonic approximation will be briefly presented. (for more details cf. ref. 7).

The potential energy ϕ_2 is assumed to be a quadratic function of the atomic displacements u_{ion} , where n refers to n th Wigner-Seitz cell, a to the a th atom in the unit cell and i distinguishes the three components of the displacement vector

$$\phi_2 = \frac{1}{2} \sum_{ion} \phi_{ion}^{i'a'n'} u_{ion} u_{i'a'n'} \quad (1)$$

$\phi_{ion}^{i'a'n'}$ are the second-order interactomic coupling parameters.

The kinetic energy of the crystal is

$$\Psi = \left(\frac{1}{2} \right) \sum_{i \in n} \frac{p_{i \in n}}{2 M_a} \quad (2)$$

$p_{i \in n}$ is the i th component of the momentum of the a th atom in cell n , and M_a is the mass of this atom.

The Hamiltonian of the crystal is then

$$H_2 = \Phi_2 + \Psi \quad (3)$$

The displacement $u_{i \in n}$ and momentum $p_{i \in n}$ can be written as a sum of waves with wave vector \vec{k} , polarization j , travelling in the $\vec{x}(k)$ direction.

$$u_{i \in n} = \sum_{k \in j} \left[\frac{\hbar}{2NM_a \omega(kj)} \right]^{\frac{1}{2}} e_{ia}^{+}(kj) [a(kj) - a^{+}(-kj)] e^{2\pi i \vec{k} \cdot \vec{x}(n)} \quad (4)$$

$$p_{i \in n} = -i \sum_{k \in j} \left[\frac{\hbar M_a \omega(kj)}{2N} \right]^{\frac{1}{2}} e_{ia}^{+}(kj) [a(kj) + a^{+}(-kj)] e^{2\pi i \vec{k} \cdot \vec{x}(n)} \quad (5)$$

e_{ia} is the polarization vector, N the total number of unit cells. $a^{+}(kj)$ and $a(kj)$ are the creation and annihilation operators.

It can be shown that the Hamiltonian takes the simpler form

$$H_2 = \sum_{k \in j} \hbar \omega(kj) [a^{+}(kj) a(kj) + \frac{1}{2}] \quad (6)$$

The sum over k is extended over the first Brillouin zone.

The eigenvalues of the Hamiltonian H_2 gives the energy of the crystal

$$E = \sum_{k \in j} [N(kj) + \frac{1}{2}] \hbar \omega(kj) \quad (7)$$

which can be interpreted as the sum of the partial energies $E(kj) = [N(kj) + \frac{1}{2}] \hbar \omega(kj)$ of each mode k and polarization j . $N(kj)$ is an integer. In term of phonons it indicates the number of phonons with energy $\hbar \omega(kj)$ in each partial wave.

2) Anharmonicity

In the harmonic approximation the various lattice waves, or phonons, are independant and there is no transfert of energy between them. Therefore a sound wave, which corresponds to a given lattice wave with a large number of phonons, will not be attenuated.

a) Landau-Rumer theory

Anharmonicities can be introduced by means of third (and/or fourth) order interatomic coupling parameters. In quantum mechanical model the anharmonic contribution to the Hamiltonian takes the form

$$H_3 = \frac{\hbar^{3/2}}{2^{3/2} 6N^{1/2}} \sum_{\substack{kk'k'' \\ jj'j''}} \frac{\phi(-kj, k'j', k''j'')}{\sqrt{\omega(kj) \omega(k'j') \omega(k''j'')}} a^+(kj) a(k'j') a(k''j'') \quad (8)$$

+ all other possible combinations of the a and a^+ operators.

These three phonon interactions must verify the energy and momentum conservation laws.

The sound wave can be considered as a lattice wave of mode KJ in which phonons are added so that their number $N(kj)$ is in excess of the thermal equilibrium number $n(kj)$. The rate at which phonons are scattered out of this mode enables to define a lifetime $\tau(KJ)$ given by

$$\frac{1}{\tau(KJ)} = - \frac{1}{N(KJ) - n(KJ)} \frac{dN(KJ)}{dt} \quad (9)$$

If $s(KJ)$ is the phase velocity of the wave the attenuation α is $\alpha = 1/2 \tau s$.

The rate of change $dN(KJ)/dt$ can be calculated by using the Golden Rule of the perturbation theory.

The anharmonic coupling also perturbs the energy levels of the sound wave. This perturbation is calculated by using the standard second-order-time-independent perturbation theory.

The validity of this method can be evaluated by considering that the thermal phonons have a finite life time. Let τ be its average. In account of the Uncertainty Principle this finite lifetime makes the phonon energy uncertain

by an amount of the order of \hbar/τ . Therefore the method will not be valid as soon as the energy uncertainty is comparable to the sound wave phonon energy $\hbar\Omega$. Thus the Landau-Rumer method is valid when $\hbar\tau \ll \hbar\Omega$, or $\Omega\tau \gg 1$. This condition is satisfied for sound waves at high frequencies or at low temperatures.

b) Akhieser Theory

At higher temperatures the thermal phonon lifetime decreases. As a consequence their mean free path becomes smaller than the sound wave length λ . The phonons can be considered as localized wave packets. The thermal phonon averaged frequency at temperature T is $k_B T/\hbar$ (k_B : Boltzmann constant). If ℓ is the wave packet length, the condition $\ell \ll \lambda$ is equivalent to $\hbar\Omega \ll k_B T$.

In this case the method proposed by Akhieser consists in using a macroscopic model for the sound wave and the microscopic one for the thermal phonons. The anharmonicities are introduced by means of a strain dependance of the phonon frequencies. A detailed description of the method can be found in ref (8).

The total energy of the crystal of volume V is the sum of the energy of the thermal phonons

$$E_{th} = \sum_{kj} (N(kj) + \frac{1}{2}) \hbar \omega(kj) \quad (10)$$

and of the mechanical potential energy due to the strains induced by the sound wave

$$E_{sound} = C_{\alpha\beta} n_{\alpha\beta} + \frac{1}{2} C_{\alpha\beta\gamma\delta} n_{\alpha\beta} n_{\delta\gamma} + \dots \quad (11)$$

$C_{\alpha\beta}$ and $C_{\alpha\beta\gamma\delta}$ have the dimension of elastic constants.

The derivative of the total energy with respect to strain gives the stress

$$T_{\alpha\beta} = (\partial/\partial n_{\alpha\beta}) (E_{th} + E_{sound}) \quad (12)$$

- When in equilibrium the number of phonons in mode kj is given by the Bose-Einstein distribution

$$n(kj) = \{\exp [\hbar \omega(kj) / k_B T] - 1\}^{-1} \quad (13)$$

and this equilibrium corresponds also to $T_{\alpha\beta} = \eta_{\alpha\beta} = 0$.

This enables to determine completely the stress

$$T_{\alpha\beta} = C_{\alpha\beta\gamma\delta} \eta_{\gamma\delta} + \frac{1}{V} \sum_{kj} [N(kj) - n(kj)] \hbar \frac{\partial \omega(kj)}{\partial \eta_{\alpha\beta}} + \frac{1}{V} \sum_{kj} [n(kj) + \frac{1}{2}] \hbar \frac{\partial^2 \omega(kj)}{\partial \eta_{\alpha\beta} \partial \eta_{\gamma\delta}} \quad (14)$$

The mechanical equilibrium equation

$$\rho \frac{\partial^2 u_{\beta}}{\partial t^2} = \frac{\partial T_{\alpha\beta}}{\partial x_{\alpha}} \quad (15)$$

and the strain-displacement relation

$$\eta_{\alpha\beta} = (\frac{1}{2}) \left(\frac{\partial u_{\alpha}}{\partial x_{\beta}} + \frac{\partial u_{\beta}}{\partial x_{\alpha}} \right) \quad (16)$$

enables to calculate plane waves solutions with wave vector K and frequency Ω

$$u_{\beta} = u_0 e_{\beta}(KJ) e^{i(2\pi \vec{K} \cdot \vec{x} - \Omega t)} \quad (17)$$

$$N(kj) = n(kj) + \Delta N(kj) e^{i(2\pi \vec{K} \cdot \vec{x} - \Omega t)} \quad (18)$$

In the absence of phonons the solution has the simpler form

$$u_{\beta} = u_0 e_{\beta}(KJ) e^{i(2\pi \vec{K} \cdot \vec{x} - \Omega_0 t)} \quad (19)$$

The correction due to the phonons can be calculated by using a perturbation method. This leads to

$$\begin{aligned} \Omega &= \Omega_0 + \frac{2\pi^2 \hbar}{\rho V \Omega_0} e_{\alpha}(KJ) e_{\gamma}(KJ) K_{\beta} K_{\delta} \sum_{kj} \frac{\partial^2 \omega(kj)}{\partial \eta_{\alpha\beta} \partial \eta_{\gamma\delta}} [n(kj) + \frac{1}{2}] \\ &\quad - \frac{\pi i \hbar}{\rho V \Omega_0} e_{\alpha}(KJ) K_{\beta} \sum_{kj} \frac{\partial \omega(kj)}{\partial \eta_{\alpha\beta}} \frac{\Delta N(kj)}{u_0} \end{aligned} \quad (20)$$

- The attenuation α is given by

$$\alpha = - \text{Im} \frac{\Omega}{s_0(KJ)} \quad (21)$$

and the new velocity of the sound wave

$$s = \text{Re} \frac{\Omega}{2\pi K} \quad (22)$$

These quantities are completely determined when $\Delta N(kj)$ is known. This corresponds to the calculation of the response of the phonon system to the sound wave, which is given by the Boltzmann equation

$$\frac{\partial N(kj)}{\partial t} = \frac{1}{2\pi} \frac{\partial \omega(kj)}{\partial n_{\alpha\beta}} \frac{\partial n_{\alpha\beta}}{\partial x_\gamma} \frac{\partial N(kj)}{\partial k_\gamma} - v_\alpha(kj) \frac{\partial N(kj)}{\partial x_\alpha} + \left[\frac{\partial N(kj)}{\partial t} \right]_{\text{coll}} \quad (23)$$

Remark : The term $\left[\frac{\partial N(kj)}{\partial t} \right]_{\text{coll}}$ is most important because it takes into account the collisions between phonons. Without collisions and with $\Omega \tau \gg 1$ and $\Omega \ll k_B T/\hbar$ the present theory goes back to the Landau-Rumer theory.

Three different types of collisions can be distinguished :

- Normal processes (N), in which quasimomentum and energy of thermal phonons are conserved in three phonon collisions

$$hk = hk' + hk'' \quad (24)$$

$$\hbar\omega = \hbar\omega' + \hbar\omega'' \quad (25)$$

Total energy and total quasimomentum also are conserved. Therefore

$$\sum_{kj} \left[\frac{\partial N(kj)}{\partial t} \right]_{\text{coll}} \hbar\omega(kj) = 0 \quad (26)$$

$$\sum_{kj} \left[\frac{\partial N(kj)}{\partial t} \right]_{\text{coll}} hk = 0 \quad (27)$$

The result of N processes is a distribution law which has the form

$$N_N(kj) = (e^{[\hbar\omega(kj) - \hbar\tilde{v}k]/k_B T_{\text{L}} - 1})^{-1} \quad (28)$$

where \tilde{v} and T_{L} are such that the conservation equations are satisfied.

- Umklapp processes (U)

The quasimomentum is not conserved

$$hk = hk' + hk'' + hg \quad (29)$$

$$\hbar\omega = \hbar\omega' + \hbar\omega'' \quad (30)$$

where g is a non zero reciprocal lattice vector.

Therefore only the total energy is conserved

$$\sum_{kj} \left[\frac{\partial N(kj)}{\partial t} \right]_{\text{coll}} \hbar\omega(kj) = 0 \quad (31)$$

and the distribution function becomes

$$N_o(kj) = \left(e^{\frac{\hbar\omega(kj)}{k_B T} - 1} \right) \quad (32)$$

- Elastic scattering (E)

It corresponds to collisions with defects and impurities, involving two phonons. The only conservation law is $\hbar\omega = \hbar\omega'$. Therefore the total energy is conserved, but also the number of phonons of any particular frequency

$$\sum_{kj} \left[\frac{\partial N(kj)}{\partial t} \right]_{\text{coll}} \delta[\omega - \omega(kj)] = 0 \quad (33)$$

The distribution function is

$$N_E(kj) = \left(e^{\frac{\hbar\omega(kj)}{k_B T(\omega(kj))} - 1} \right) \quad (34)$$

In the case of U processes, of N processes with some E and U processes (necessary to give a redistribution of the quasimomentum), or of E processes with some N and U processes (also to bring the phonon distribution to equilibrium) attenuation and velocity take the general form

$$\alpha = \frac{CT\Omega_o \gamma^2}{2\omega_o^3} \frac{\Omega_o \tau}{1 + \Omega_o^2 \tau^2} \quad (35)$$

$$s - s_o = \frac{CT\gamma^2}{2\omega_o^3} \frac{\Omega_o^2 \tau^2}{1 + \Omega_o^2 \tau^2} \quad (36)$$

where γ is an effective Grueneisen constant depending on the nature of the process involved, C the specific heat ; and τ the mean relaxation time of the thermal phonons.

Introducing the low frequency young modulus $E_0 = \rho s_0^2$, the quantity $\Delta E = CTY^2$ and, the relation between attenuation and Q-factor $a = \Omega_0/(2Qs_0)$, and between velocity and frequency $(s-s_0)/s_0 = (\Omega-\Omega_0)/\Omega_0$ one obtains

$$\frac{1}{Q} = \frac{\Delta E}{E_0} \frac{\Omega_0 \tau}{1 + \Omega_0^2 \tau^2} \quad (37)$$

In the case of a resonator fluctuation $\delta\tau$ in the relaxation time τ will produce a fractional frequency fluctuation $y = \delta\Omega/\Omega_0$ of the resonator frequency

$$y = \frac{\Delta E}{E_0} \frac{\Omega_0^2 \tau^2}{(1 + \Omega_0^2 \tau^2)} \frac{\delta\tau}{\tau} \quad (39)$$

In terms of power spectral densities $S_y(F)$ and $S_{\delta\tau/\tau}(F)$ and using the relation (37) in (39) one obtains

$$S_y(F) = \frac{1}{Q} \left(\frac{E_0}{\Delta E} \right)^2 S_{\delta\tau/\tau}(F) \quad (40)$$

This relation shows the $1/Q^4$ law which was observed experimentally, between the noise levels and the Q-factors.

For higher values of $\Omega_0 \tau$ the Landau-Rumer method must be used. At the present state of this study the frequency change at low temperature was not calculated yet. Only attenuation was evaluated.

Near room temperature attenuation is proportional to T as shown by relation (35). At low temperature it becomes proportional to T^4 . This corresponds to what is observed experimentally, even if the attenuation behavior is sometimes closer to T^4 or T^6 . The difference can be explained by the temperature dependence of τ , which does not appear explicitly in the relations.

However temperature also appears in relation (40) in both Q and E . When T decreases, Q increases and therefore there is some compensation in the product $Q^4 E^2$. This can explain why the three experimental points of table I corresponding to $1/F$ noise levels at $300^\circ K$, $4.2K$ and $1K$ does not strictly follow the $1/Q^4$ law.

CONCLUSION

The experimental results obtained during this study shown for the first time a correlation between 1/F noise and Q-factor in quartz crystal resonators.

This dependance was confirmed on the one hand by low temperature measurements and on the other hand by a theoretical model.

This theory based on phonon interactions is a first approach to a more general theory of flicker noise. For this purpose it will be necessary to precise the fluctuation spectrum of the phonon relaxation time, and calculate the frequency shift at low temperature by using the Landau-Rumer theory, in order to introduce completely the temperature dependance in the model.

For a practical point of view, the large increase of Q-factor and the lower noise levels open the possibility of achieving cryogenic quartz crystal oscillators with better stability.

References

- (1) G. Théobald, G. Marianneau, R. Prétot, J.J. Gagnepain, "Dynamic thermal behavior of quartz resonators", 33rd An. Freq. Cont. Symp., Fort Monmouth, 1979.
- (2) G. Marianneau, J.J. Gagnepain, "Digital temperature control for ultrastable quartz oscillators", 34th An. Freq. Cont. Symp., Fort Monmouth, 1980.
- (3) A.E. Wainwright, F.L. Walls, W.D. McCaa, "Direct measurements of the inherent frequency stability of quartz crystal resonators", 28th An. Freq. Cont Symp., Fort Monmouth, 1974.
- (4) J.J. Gagnepain, "Fundamental noise studies of quartz crystal resonators", 30th An. Freq. Cont. Symp., Fort Monmouth, 1976.
- (5) L. Landau, G. Rumer, Phys. Z. Sowjetunion 11, 18, 1937.
- (6) A. Akhieser, "On the absorption of sound in solids", J. Phys. (USSR), 1, 277, 1979.
- (7) O. Madelung, "Introduction to Solid-State Theory", Springer-Verlag, 1978.
- (8) H.J. Maris, "Interaction of sound waves with thermal phonons in dielectric crystals", Physical Acoustic, vol. VIII, Academic Press, 1971.
- (9) J. Uebersfeld, Private Communication.

II - FAST WARM-UP SAW OSCILLATOR

GENERAL PRESENTATION

The characteristics of surface acoustic waves are modified by temperature variations. These external effects are at the origin of the main causes of frequency instabilities in SAW oscillators.

When the temperature fluctuations are slow enough, the thermal distribution in the volume of the crystal is uniform. The usual model using a polynomial expansion up to the third order versus temperature is satisfactory to describe the static thermal behavior. For faster temperature variations a spatial distribution of temperature within the crystal arises. Consequently, thermal effects involve temperature gradients which induce thermal stresses and strains. This is the "Dynamic thermal behavior"⁽¹⁾⁽²⁾. These thermal stresses and strains are coupled with the surface wave by the intrinsic and induced nonlinearities of the substrate. Velocity and frequency shift follow.

The present work shows that

- the fast temperature variations induce frequency changes which are proportional to the time derivative of the internal temperature.
- the measured ST-cut dynamic temperature coefficient $\tilde{\alpha}_{ST}$ is equal to $2.10^{-5} \text{ s}/\text{°K}$ and is comparable to the coefficient of the AT-cut quartz crystal bulk wave resonator ($1.3.10^{-5} \text{ s}/\text{°K}$).
- the measured dynamic TC's of doubly rotated cuts are larger in SAW than in BAW oscillators.

The theoretical study was composed of

- calculation of the temperature distributions and corresponding thermal stresses and strains by taking into account the mechanical mounting of the SAW device.
- calculation of the dynamic T.C. $\tilde{\alpha}$ by using a perturbation method applied to the general model of an acoustic wave propagating in a strained medium.

The measurements of the dynamic thermal behavior required a temperature controlled oven operated by means of a computer. Numerical programs enable to perform given temperature cyclings. From the corresponding frequency responses the $\tilde{\alpha}$ -coefficient are deduced.

TEMPERATURE DISTRIBUTION

A unidimensional model has been used. It consists in a crystal plate of $2h$ -thickness and of infinite lateral sizes along a_1 and a_3 (fig. 1).

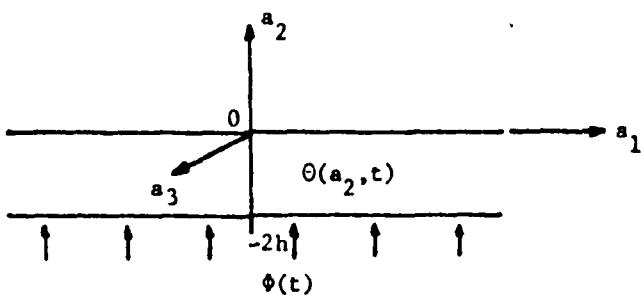


Fig. 1 : Temperature distribution

A more accurate model should take into account the influence of the force at the fixation points under the crystal thermal expansion. Only the bottom of the plate was submitted to temperature variations $\Phi(t)$.

Let $\theta(a_2, t)$ be the temperature inside the crystal. The boundary conditions are

$$\theta(-2h, t) = \Phi(t) \quad \text{and} \quad \theta(0, t) = 0 \quad (1)$$

The heat transfer with the surrounding medium on the propagation surface ($a_2 = 0$) is considered to be very fast.

Consequently, temperature distribution within the crystal follows the general relation given by H. Carslaw ⁽³⁾

$$\theta(a_2, t) = \sum_{n=1}^{\infty} \frac{n\pi k}{2h^2} \exp \left\{ -\frac{n^2 \pi^2 k t}{4h^2} \right\} \sin \frac{n\pi a_2}{2h} I(t) \quad (2)$$

with

$$I(t) = \int_0^t \exp \left\{ \frac{n^2 \pi^2 \kappa \lambda}{4h^2} \right\} (-1)^n \Phi(\lambda) d\lambda \quad (3)$$

where K is the thermal diffusivity constant of the crystal in the a_2 direction.

Considering that $\Phi(t)$ is a slowly varying function of time, the integration of $I(t)$ has been performed by parts, and the time derivatives higher than the first order neglected.

Then, the temperature distribution is given by

$$\theta(a_2, t) = -\frac{a_2}{2h} \Phi(t) + \frac{1}{3\kappa} \left(-\frac{a_2^3}{4h} + a_2 h \right) \dot{\Phi}(t) \quad (4)$$

$\dot{\Phi}(t)$ is the first time derivative of $\Phi(t)$

$$\dot{\Phi}(t) = \Phi(t), t \quad (5)$$

The internal temperature $\theta(a_2, t)$ having a spatial distribution, thermal stresses and strains appear. By following Holland ⁽⁴⁾, the adiabatic deformation \underline{n}_{ij} which takes place, is given by the following relations written in the material reference system.

$$[\underline{n}_N] = A_N a_2 + B_N \quad (6)$$

with $N = 1, 3, 5$

and

$$[\underline{n}_Z] = \theta(a_2, t) [a'_Z] - [c_{ZZ}]^{-1} [c_{ZN}] [\underline{n}_N] \quad (7)$$

with $Z = 2, 4, 6$

The different coefficients are given by the relations

$$A_N = \frac{12}{(2h)^3} (\bar{a}h + \theta) \quad (8)$$

$$B_N = \frac{12}{(2h)^2} \left(\bar{\theta} \frac{2h}{3} + \hat{\theta} \frac{h}{2} \right) \quad (9)$$

$$[\alpha'_Z] = [\alpha_Z] + [C_{ZZ}]^{-1} [C_{ZN}] [\alpha_N] \quad (10)$$

$$\bar{\theta} = \int_{-2h}^0 \theta(a_2, t) da_2 \quad (11)$$

$$\hat{\theta} = \int_{-2h}^0 \theta(a_2, t) a_2 da_2 \quad (12)$$

where α_Z and α_N are the thermal dilatation constants and $[C]$ are the elastic constants.

By using the stress-strain relations, tensions t_{ij} induced by the deformations and the temperature distribution, are calculated (also in the matricial reference system)

$$[t_N] = ([C_{NN}] - [C_{NZ}][C_{ZZ}]^{-1}[C_{ZN}]) ([\alpha_N] - [\alpha_N] \theta(a_2, t)) \quad (13)$$

and $[t_Z] = 0 \quad (14)$

in account of the boundary conditions corresponding to a plate which is free to expand.

FREQUENCY SHIFTS

Considering the temperature variations as a bias applied to the crystal, propagation properties are modified and in a natural state coordinate system the nonlinear propagation equation is written

$$\rho_0 u_{i,tt} = (\overline{A_{ikjm}} u_{j,m})_k \quad (15)$$

where ρ_0 is the specific mass and u_j the displacement due to the high frequency vibrations.

The boundary conditions corresponding to a stress free surface are

$$\overline{A_{ikjm}} u_{j,m} = 0 \quad \text{for } a_2 = 0 \quad (16)$$

where \overline{A}_{ikjm} are the modified elastic constants, which can be written in the form

$$\overline{A}_{ikjm} = \overline{C}_{ikjm} + \overline{H}_{ikjm} \quad (17)$$

where the \overline{H}_{ikjm} tensor is considered as a small term with respect to the second order elastic constant \overline{C}_{ikjm} . It can be related to the temperature and the thermal stresses and strains in the following way

$$\overline{H}_{ikjm} = \overline{\delta}_{ij} \overline{t}_{km} + \overline{U}_{i,p} \overline{C}_{kpmj} + \overline{U}_{j,q} \overline{C}_{kimq} + \overline{n}_{uv} \overline{C}_{kmpquv} + \alpha_{\overline{C}_{ikjm}} \overline{C}_{ikjm} \theta(a_2, t) \quad (18)$$

where \overline{t}_{km} , \overline{n}_{uv} and $\overline{U}_{i,p}$ are respectively the thermodynamic tensions, the deformations and the displacement gradients. Here, $\alpha_{\overline{C}_{ikjm}}$ is the first order temperature coefficient of elastic constants for the considered-cut.

In the case of SAW oscillators, the nonlinear coupling of the crystal with the high frequency wave depends on its depth penetration. Then perturbation terms \overline{H}_{ikjm} are function of the step variable a_2 and can be written following the relation :

$$\overline{H}_{ikjm} = \sum_n \alpha_{ikjm}^{(n)} a_2^n \quad (19)$$

By using a perturbation method ⁽⁵⁾, relative frequency shifts are calculated

$$\frac{\Delta\omega}{\omega_c} = \frac{\sum_n \left[\sum_{p,q} \frac{\overline{A}_p \overline{u}_j^*(p) \overline{A}_q^* \overline{u}_i^*(q) \overline{n}_m^*(p) \overline{n}_k^*(q)}{q_p - q_q^*} \cdot \frac{n! \alpha_{ikjm}^{(n)}}{\left(i \frac{\omega_0}{V_0} (q_p - q_q^*) \right)^n} \right]}{2 \rho_0 V_0^2 \sum_{p,q} \frac{\overline{A}_p \overline{u}_l^*(p) \overline{A}_q^* \overline{u}_l^*(q)}{q_p - q_q^*}} \quad (20)$$

Since the temperature distribution ⁽⁴⁾ is proportional partly to $\theta(t)$ and partly to the time derivative $\dot{\theta}(t)$, the perturbation terms \overline{H}_{ikjm} have two parts

$$\overline{H}_{ikjm} = \overline{a}_{ikjm} \theta(t) + \overline{b}_{ikjm} \dot{\theta}(t) \quad (21)$$

Therefore, from relation (21) and the perturbation relation (20), the relative frequency shift becomes after integration over the active surface of the plate,

$$\frac{\Delta\omega}{\omega_0} = a\Phi(t) + \tilde{a}\dot{\Phi}(t) \quad (22)$$

where the a_0 -term is related to the first order temperature coefficient of the frequency (static thermal behavior) and \tilde{a} is the dynamic temperature coefficient. Theoretical results are presented in table I for different quartz-cuts.

Table I
Values of the dynamic thermal coefficient \tilde{a} for different orientations
of quartz-crystal

Crystal Cuts	ST,X	AT,X	Y,X	$\phi = 6^\circ 20'$ $FST \theta = -41^\circ 30'$ $\psi = 26^\circ$
\tilde{a} in 10^{-6} S/°K	0.04	-1.4	-3.5	2.8
ratio $\left(\frac{\tilde{a}_{cut}}{\tilde{a}_{ST}} \right)$	1	-35.0	-87.5	70.0

TEMPERATURE CONTROLLED OVEN

SAW delay lines built with different cuts of quartz crystal were submitted to temperature cyclings by using a temperature controlled oven (6). As shown in figure 2, SAW devices and a LC-cut quartz temperature probe are mounted in the same oven. Temperature is measured with a quartz thermometer and controlled by a computer which drives the oven by comparing the measured temperature with a reference temperature. The temperature follows a variation law given by a program included in the computer. Sinusoidal cyclings can be realized with an accuracy of a few 0.001°C , as the SAW oscillator frequency is measured.

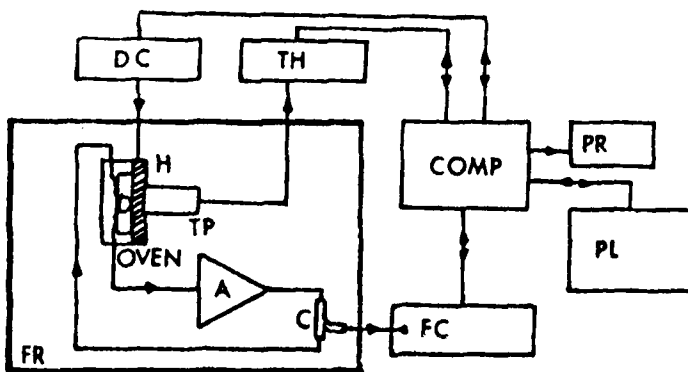


Figure 2. Temperature controlled oven.
D: SAW delay line; H: Heater;
TP: Temperature probe;
A: Amplifier; C: Directional
coupler; DC: D.C. power supply;
TH: Thermometer; FC: Frequency
counter; COMP: Computer;
PR: Printer; PL: Plotter;
FR: Freezer.

EXPERIMENTAL RESULTS

Figure 3 shows an experimental curve obtained by sweeping temperature over a temperature range of 4°C about 15°C with sweep frequency of $2.3 \cdot 10^{-4}$ Hz for a regular ST-cut fixed in two points by epoxy on a flat heater. The measured dynamic temperature coefficient is equal to $+2 \cdot 10^{-5}$ S/°K and is significantly larger than the theoretical one. The oscillator frequency was 87.8 MHz. The same plate was submitted to temperature cyclings applied on one end by a second heat source. Thus more inhomogeneous temperature distributions are introduced and the measured dynamic temperature coefficient obtained is ten times greater than the previous one ($-2 \cdot 10^{-4}$ S/°K).

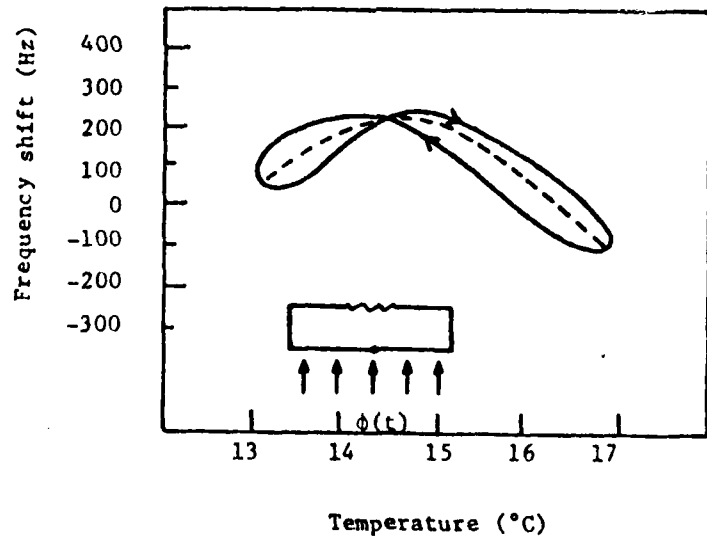


Fig. 3 -Experimental sinusoidal temperature cycling. Sweep frequency: $2.3 \cdot 10^{-4}$ Hz, ST-Cut $\Delta\theta: \pm 2^\circ\text{K}$ about $15^\circ\text{C} - f_{13^\circ\text{C}} = 87.8$ MHz.
---Static frequency-temperature characteristic.

Figure 4 presents the experimental curve obtained with temperature cycling for regular mounting of doubly rotated cut, called PFT-cut ($\Theta = 62.0^\circ$, $\Phi = 41.0^\circ$, $\Psi = 26^\circ$) which has a first order static temperature coefficient equal to zero at 5780, the second order being twice smaller than that for the PT-cut one (61). The temperature range is 40°C about 56°C and the sweep frequency is also $2.3 \cdot 10^{-4}$ Hz. Measured dynamic temperature coefficient is $2.1 \cdot 10^{-4}$ K/K, larger than the corresponding theoretical one. The oscillation frequency was 176.7 MHz at 2050.

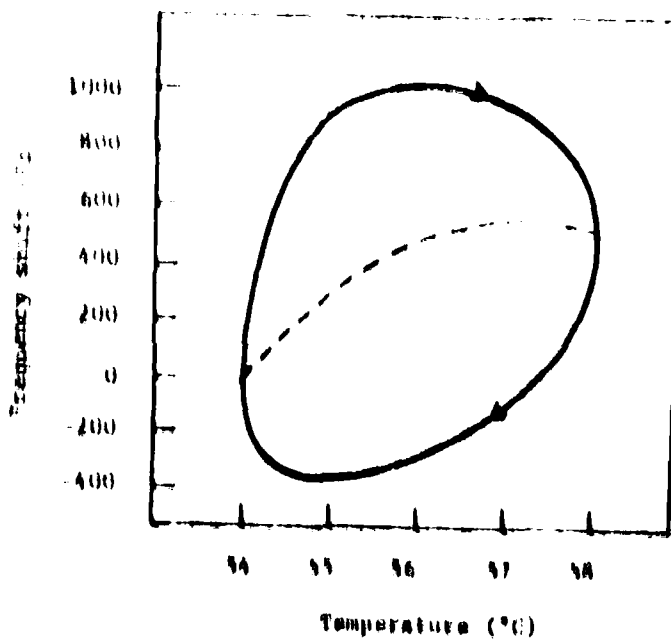


Fig. 4 - Experimental sinusoidal temperature cycling sweep
 frequency $2.3 \cdot 10^{-4}$ Hz. PFT-cut ($\Theta = 62.0^\circ$,
 $\Phi = 41.0^\circ$, $\Psi = 26^\circ$) $\Delta 0 = \pm 2^\circ\text{K}$ about 56°C
 $f_{M,0} = 176.7 \text{ MHz}$
 --- static frequency-temperature characteristic.

The large difference between theoretical and measured values is certainly due to the one-dimensional heat diffusion model which does not take into account the thermal distribution following η_1 -axis and also edge conditions at holder points. In any case, the difference between measured ratio of dynamic temperature coefficient of PFT-cut and PT-cut and the theoretical one is small.

CONCLUSION

The value of the dynamic T.C. $\tilde{\alpha}$, obtained from the experimental frequency responses is equal to 2.10^{-5} s/ $^{\circ}$ K for ST-cut quartz SAW oscillator. This coefficient is comparable to the $\tilde{\alpha}$ of AT-cut quartz BAW oscillator ($1.3.10^{-5}$ s/ $^{\circ}$ K). But this dynamic thermal behavior can be modified by changing the mounting of the substrate in order to minimize the stress effects.

The theoretical model must be improved :

- by introducing the heat exchange by radiation
- by using a bidimensional model which will take into account the edge conditions.

This first study enabled to determine the order of magnitude of the SAW dynamic thermal effect and to make comparison with bulk waves.

The continuation will consist in improving the theoretical model to study the influence of crystal orientation and wave propagation direction on the α coefficient and determine if doubly rotated cuts can be used with minimized dynamic effect.

REFERENCES

- (1) G. Théobald, G. Marianneau, R. Prétot, J.J. Gagnepain, "Dynamic thermal behavior of quartz resonators", 33rd An. Freq. Cont. Symp., Fort Monmouth, 1979.
- (2) A. Ballato and J. Vig, "Static and dynamic frequency-temperature behavior of singly and doubly rotated, oven controlled quartz resonators", Proc. 32nd An. Freq. Cont. Symp., Fort Monmouth, 1978.
- (3) H. Carslaw and J. Jaeger, "Conduction of heat in solids", Oxford University Press, London, 1959.
- (4) R. Holland, "Non uniformly heated anisotropic plates : II. Frequency transients in AT and BT quartz plates", Ultrasonics Symp. Proc., IEEE cat. 74 CHO 896-1SU (1974).
- (5) D. Hauden, "Etude des propriétés non linéaires des ondes élastiques de surface : applications aux oscillateurs et aux capteurs à quartz", Thèse Besançon, 1979.
- (6) D. Hauden, G. Théobald, "Dynamic thermal sensitivity of SAW quartz oscillators", IEEE Ultrasonics Symposium Proceedings, 1980.

MISSION
of
Rome Air Development Center

RADC plans and executes research, development, test and selected acquisition programs in support of Command, Control Communications and Intelligence (C³I) activities. Technical and engineering support within areas of technical competence is provided to ESD Program Offices (POs) and other ESD elements. The principal technical mission areas are communications, electromagnetic guidance and control, surveillance of ground and aerospace objects, intelligence data collection and handling, information system technology, ionospheric propagation, solid state sciences, microwave physics and electronic reliability, maintainability and compatibility.

